Thermal perturbation, mineralogical assemblages and rheology variations induced by dyke emplacement in the crust

A. LAVECCHIA(1,2), S.R. CLARK(1), F. BEEKMAN(2) & S. CLOETINGH(2)
(1)Simula Research Laboratory, Martin Linges vei 17 Fornebu, Norway; (2)Utrecht University, Utrecht, The Netherlands *alessio@simula.no*

[simula . research laboratory]

1 – Introduction and model features

It is presented a physical model simulating thermal perturbation in a two-layered crustal section, induced by the emplacement of a sequence of basaltic dykes, and taking into account mineralogical assemblage variations. The main purpose of the work is to obtain more quantitative constrains on the interactions between temperature, mineralogical assemblage and rheology during the emplacement of melts at crustal levels. Results may be useful for the comprehension of rifting areas, where strain hardening of bodies can determine a switch between different rift mechanisms and have a primary effect on mantle decompression along the rift axis.

Solutions are obtained numerically by using FEniCS, a collection of free libraries for solving partial differential equations with the finite elements method. The model is based on a 2D geometry (Fig.1) and reproduces a 35 km thick and 50 km wide crust section, composed of a 15 km thick upper crust and a 20 km thick lower crust, thermally perturbed by a set of 10 basaltic dykes, each with a thickness of 1 km. The total thickness of the dyke set is 10 km and is reached by lateral accretion (from the right leftward) in a time interval of 10 Myr, in agreement with thickness estimated for the Main Ethiopian Rift (Bastow *et al.*, 2011). Thickness and lateral extension of the crust are assumed to be constant during the simulation.

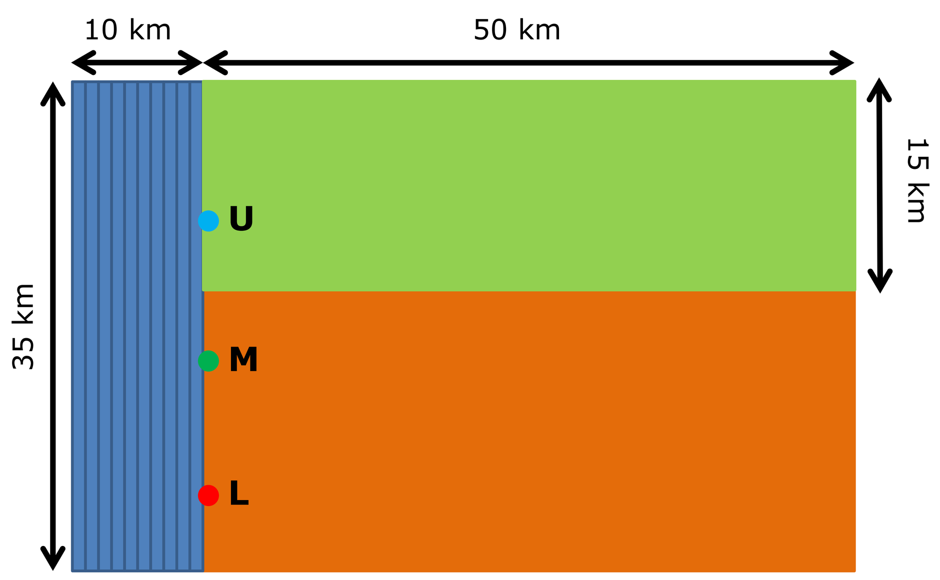

Fig. 1 – Schematic representation of the geometry reproduced by the model. The coloured dots indicate locations of points selected for T-t plots (see Fig. 3); every point is located at 100 m from the dykes-crust boundary, at a depth of 10 km (blue, **U**), 20 km (green, **M**) and 30 km (red, **L**).

2 – Metamorphism and thermal features

Metamorphism has been modelled by taking into account common minerals in metapelitic rocks (chlorite, muscovite, quartz, staurolite, allumosilicates, biotite, garnet and plagioclase) in a MnMFKASH chemical system. Compositions are assigned for the upper and lower crust and recalculated by using the reaction grid in (Fig. 2). The same reaction grid is used for dyke-induced metamorphism. Thermodynamic data are taken from (Holland & Powell, 1998) and kinetics of reaction is considered. The thermal equation adopted in the model [1]:

$$\rho c_P \frac{\partial T}{\partial t} = k(T)\frac{\partial^2 T}{\partial T^2} + H + \frac{1}{V}\frac{\partial Q}{\partial T} \qquad [1]$$

Takes into account a temperature-dependent thermal conductivity, a depth-decaying radiogenic heat production and reaction enthalpy. The model assumes a fixed heat flow from the crust base and a variable heat flow at surface, according to the Newton law of cooling. Parameters adopted in the thermal model and initial crust compositions are illustrated in (Tab. 1).
For the three case studies, different reaction kinetics have been considered, based on different garnet growth velocities. More in detail, it has been tested a thermorheological behaviour when the garnet reaction velocity is 650 mol m^{-3} yr^{-1} (fast), 350 mol m^{-3} yr^{-1} (medium) and 50 mol m^{-3} yr^{-1} (slow).
Results are presented on T-t diagrams for various locations in the crust (Fig. 3), and as contoured vertical sections at different times (Fig. 5). The stepwise emplacement of dykes result in a pulsating change of temperature on T-t plots. The first dykes produce very pronounced and short-living thermal peaks, whereas the temperature profiles smooth after the 5th dyke emplacement. If a fast reaction kinetics is considered, the differences in temperature due to metamorphism are not pronounced in these three case studies, and do not exceed 10 °C in the lower crust (Fig.3a). Values obtained by using a medium velocity kinetics are very close to those obtained by fast kinetics, although the T-t paths are slightly colder than the first ones (Fig. 3a). It may be due to the occurrence of reaction with a higher enthalpy at later simulation time, since the first reactions do not have the time to consume all the reactants needed for further reaction at higher temperature.
If a slow reaction kinetics is considered, temperature are considerably lower, especially in the bottom of the lower crust, where an extensive partial melting has been recorded. Magma produced may reach percentages of ≈30% and here the rock bodies involved may be considered as crystals-melt mush. The effect on temperatures may be observed in (Fig. 3b), where the maximum difference registered are ≈30 °C, and are due to the latent heat of fusion needed to generate muscovite and biotite dehydration melts.

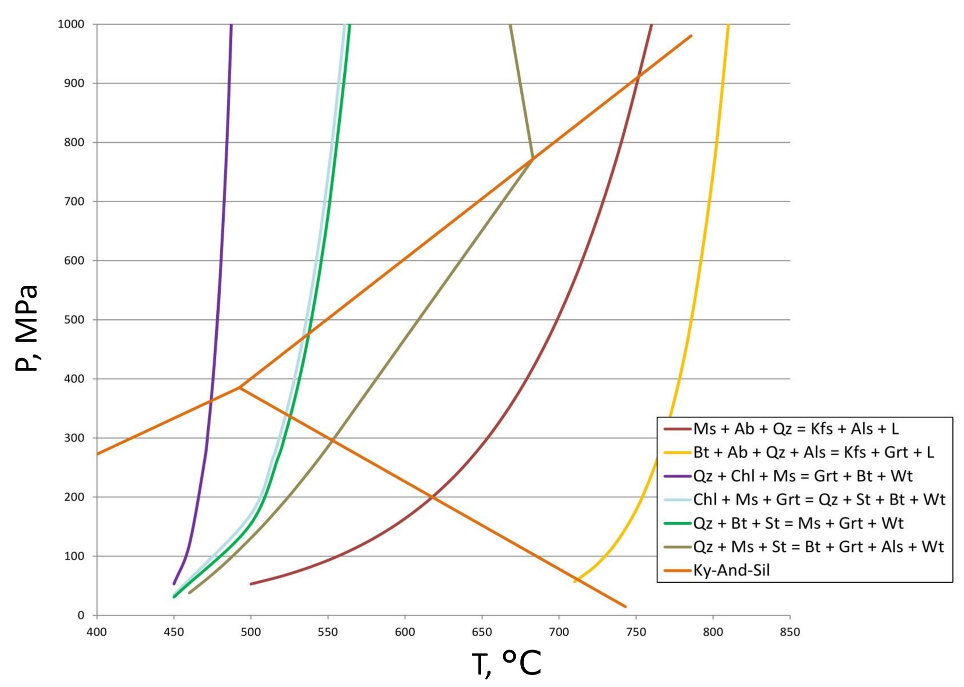

Fig. 2 – Reaction grid used to simulate metamorphism in the crust. Reactions in the label occur with increasing temperature.

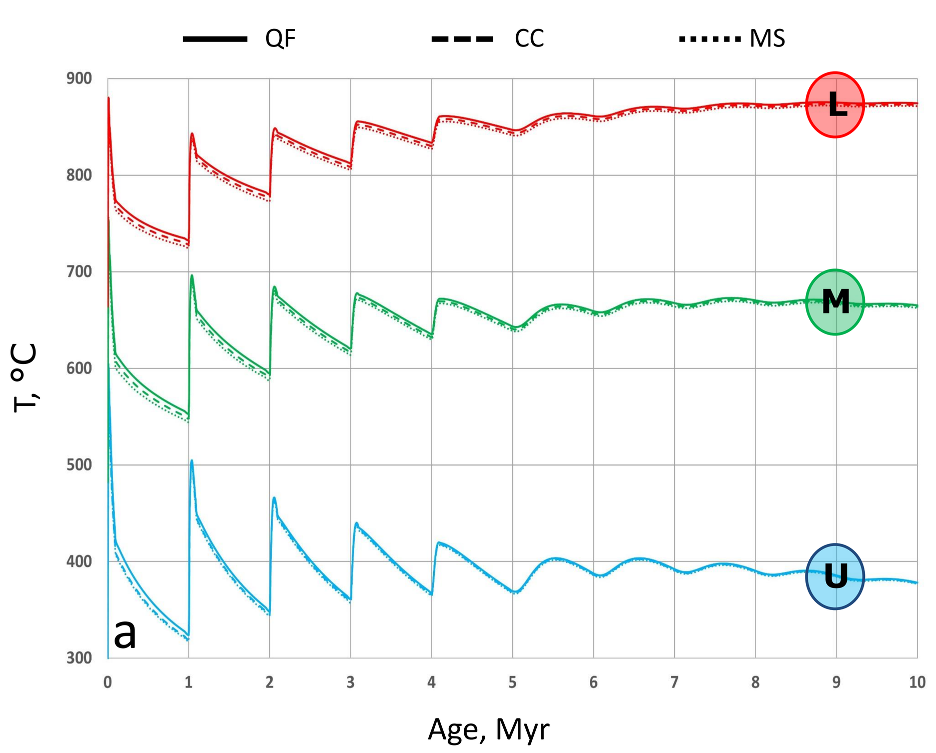

Fig. 3a - Thermal evolution in the wall rocks close to the margin of the dykes at a distance of 100 m from the contact, lasting 10 Ma from magma emplacement. The location of points related to this diagrams is shown in Fig. 1.
Temperature peaks related to the emplacement of the first dykes are pronounced and short-living, decreasing their intensity and increasing their duration progressively.
Difference in temperature are relatively greater in micaschists than in the case of mineralogical association approximating the chemical composition of the whole crust.

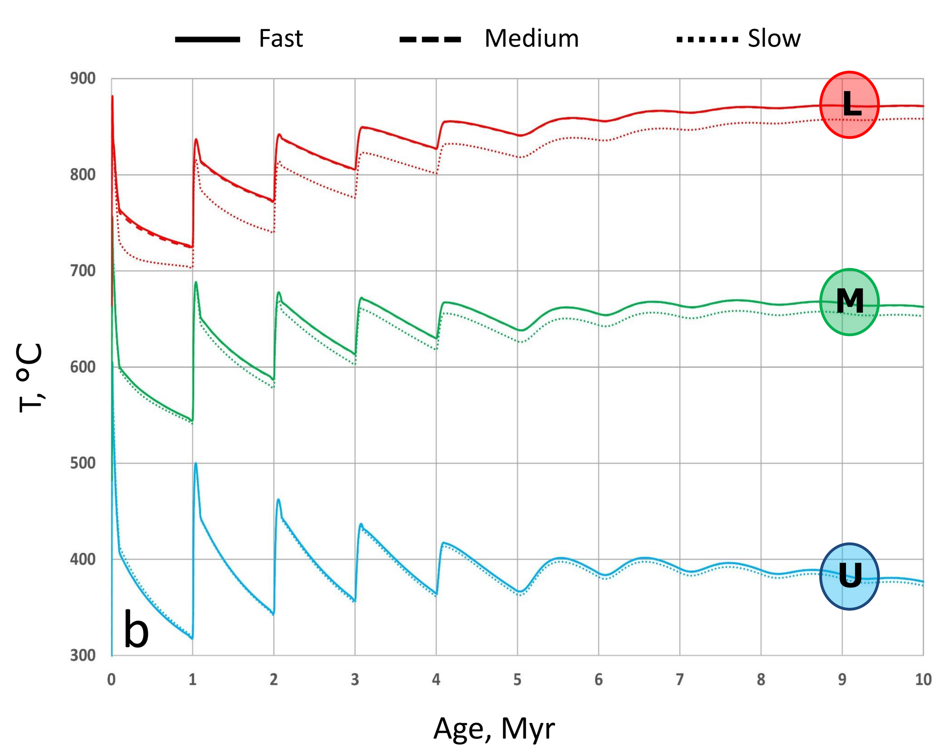

Fig. 3b - Thermal evolution in the wall rocks in the MS case study, dependent on different reaction kinetics. The location of points related to this diagrams is shown in Fig. 1.
The differences in temperature are negligible between the fast kinetics case and the medium kinetics case. In the slow kinetics case the temperature differences are observable in the [M] T-t path, and significant in the [U] T-t path.
If the CC composition is considered, the differences in temperature are smaller, although still occurring, and follow the same trend.

Surface temperature (t = 0)	25 °C	Characteristic depth	12 km
Crust base temperature (t = 0)	750 °C	Heat transfer coefficient	15 W m^{-2} K^{-1}
Magma emplacement temperature	1300 °C	Crust base heat flow	27 mW m^{-2}
Solidus temperature	1000 °C	Heat capacity	800 J kg^{-1} K^{-1}
Radiogenic heat productivity (depth = 0)	2 mW m^{-3}	Latent heat of crystallization	400 kJ kg^{-1}

Mineral assemblages:	
Quartz-Feldspars (QF)	**UC**: qz100; **LC**: fs100
Crust Geochemistry (CC)	**UC**: chl13, ms13, qz37, pl23, kfs14; **LC**: ms13, qz13, pl20, ky4, grt16, bt20, st2, kfs13
Micaschists (MS)	**UC**: chl30, ms25, qz25, pl10, kfs10; **LC**: ms10, qz20, pl15, ky5, grt10, bt25, st5, kfs10

Tab. 1 – Thermal parameters and mineral assemblages adopted in the model.

3 – Rheology plots

The modelled thermal evolution provides the framework for an estimation of the time-dependent rheological behaviour of crust with different compositions. Two-dimensional strength profiles have been obtained using the frictional criterion [2] for the brittle domain and the power-law creep equation [3] for the ductile domain:

$$\sigma = \beta\rho g z(1-\lambda) \qquad [2] \qquad\qquad \dot{\varepsilon} = A\sigma^n exp\left(-\frac{Q}{RT}\right) \qquad [3]$$

In the frictional criterion we adopt a β value of 0.75 (tectonic extension) and λ (pore fluid factor) values of 0.4. The rheological parameters values in the power-law creep equation have been estimated in the crust for every time step, following the averaging procedure for polyphase aggregates suggested by Ji et al. (2003). Values of differential stress (σ) for the single phases and relative to the power-law creep are shown in (Fig. 4). Values of differential stress obtained with the two different formulas have been compared for each grid point and then combined to obtain stress values cross-sections (Fig. 5). During this time window, a quartz-feldspatic crustal compositions is characterized by a shallowing of the brittle-ductile boundary and an extension of the ductile field. A crust characterized by mineralogical associations approximating the crust chemical compositions shows very different stress values, with a weaker upper crust and a considerably stronger lower crust. In addition, the dykes upper and middle aureole now shows a brittle behaviour and constitutes a stronger interval compared to surrounding rocks (except for a ductile spot at the bottom of the upper crust. In the micaschist crust case, almost all the dyke aureole and the upper-middle part of the lower crust show a brittle behaviour since the first moments after the simulation. In the last two cases, big rheological contrasts may favour decollément during geodynamic evolution of extensional areas. Furthermore, an increase in strength due to the presence of a metamorphic aureole next to the dykes might determine the possibility of a diversion in the dyke emplacement, or favour the switch between rifting by predominant crust thinning and by predominant magma filling.

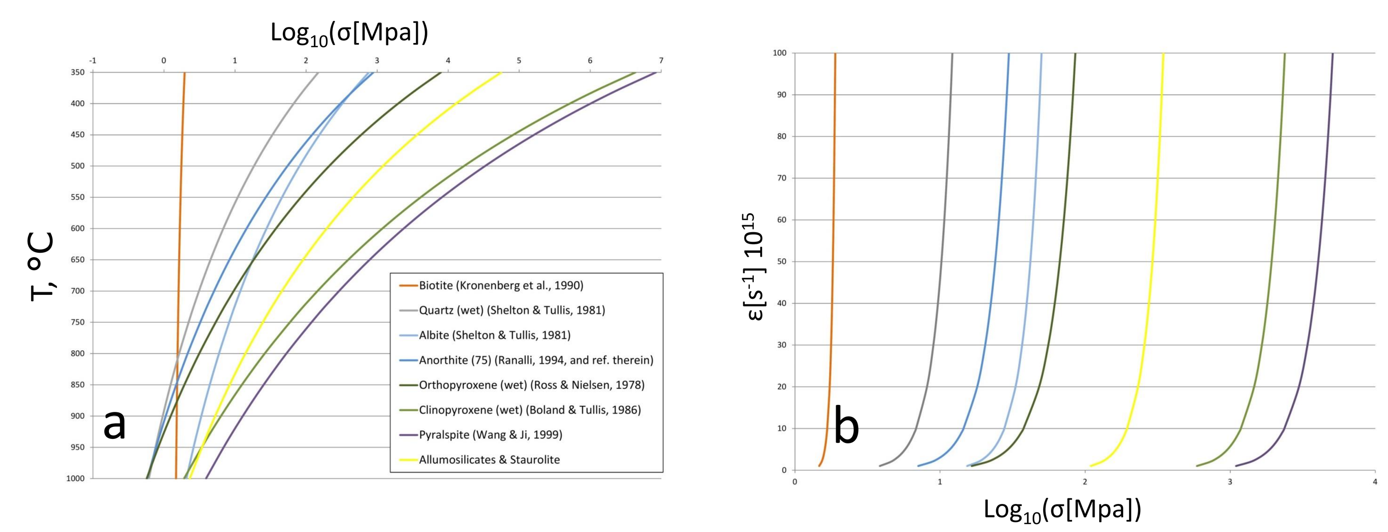

Fig. 4 – Strength plots for common minerals relative to power-law creep. **a**) Temperature-differential strength of minerals at a strain rate of 10^{-14} s^{-1}; curve for allumosilicates and staurolite is an average between rheology curves of quartz, plagioclase, pyroxene and garnet. Albite curve has been used in the simulation for feldspars, while biotite curve has been used for phyllosilicates. **b**) Strain rate-strength curves at a temperature of 600 °C; minerals show higher strength differences at values of strain rate less than $2\cdot10^{-14}$ s^{-1}.

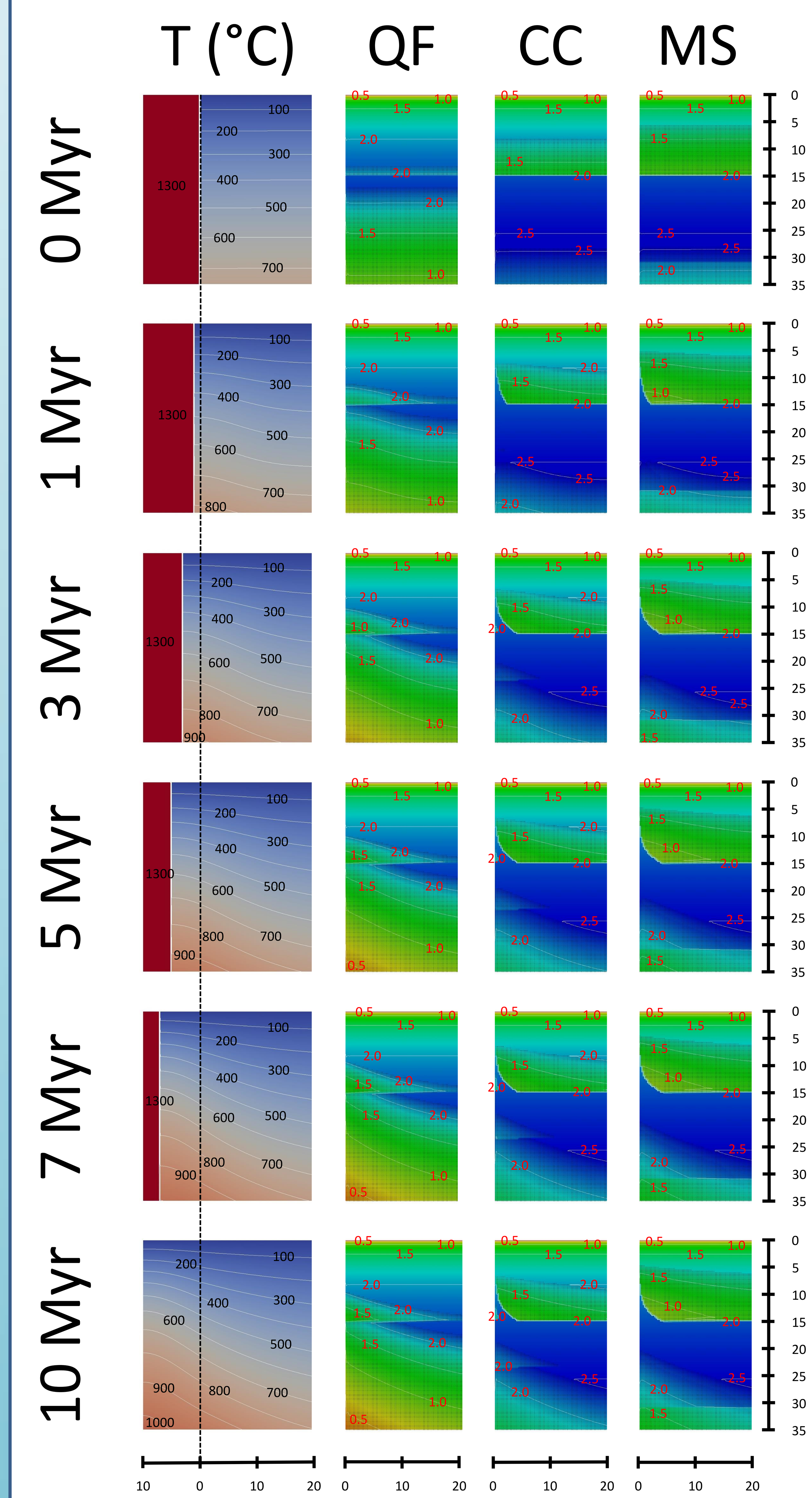

4 – Conclusions

The main results emerging from this study are the following:

1) Temperature profiles may be deeply influenced by metamorphism, depending on the initial composition and the metamorphism features. Variations registered may reach values of more than 30 °C. This effect must be considered especially in the lower crust, where temperature peaks are retained for longer periods, while they can be considered negligible (although still occurring) in the upper crust.
2) The rheology of the crust is deeply influenced by mineralogical association and its variation during time. If compared to a "classical" quartz-feldspatic (QF) crust, the other two case studies (CC and MS) show strong differences in stress values. The upper crust is weaker and the brittle-ductile transition is shallower. On the contrary, the lower crust is considerably stronger, and may be brittle for most of its thickness.
3) Crusts with micaschists mineralogy or approximating the whole crust chemical composition show strong rheology contrasts; these levels may favour strain partitioning and decoupling during the geodynamic evolution of the area.
4) An increase in strength in the areas surrounding dykes location is observable at the very early phases of emplacement and extends during the simulation. This may entail a switch in dykes emplacement location and/or favour the transition from crust thinning rifting to magma assisted rifting mechanisms.
5) If the reaction kinetics is slower, appropriate temperatures for muscovite and biotite reaction are reached before the consumption of these minerals during other metamorphic reactions. It leads to an extensive partial melting and a significant decrease in temperature, registered in the T-t path.

References

BASTOW I.D., KEIR D. & DALY E. (2011) - The Ethiopia Afar Geoscientific Lithospheric Experiment (EAGLE): Probing the transition from continental rifting to incipient seafloor spreading. From: Beccaluva L., Bianchini G. & Wilson M. (eds.), Volcanism and Evolution of the African Lithosphere. Geological Society of America Special Paper 478, 51–76.
HOLLAND T.J.B.& POWELL R. (1998) – An internally consistent Thermodynamic dataset for phases of petrological interest. J. Metamorphic Geol., 16, 309-343.
JI S., ZHAO P. & XIA B. (2003) – Flow laws of multiphase materialsand rocks from end-member flow laws. Tectonophysics, 370, 129-145.
RUDNICK R.L. & GAO S. (2003) – Composition of the continental crust. From: Holland H.D. & Turekian K.K. (eds), Treatise on geochemistry, vol.III. Elsevier, 1-64.